Seasonal inflow of warm Deep Water (WDW) in the continental shelf in the Filchner Ronne ice shelf

Tchonang Babette C.[1], Hattermann Tore [2], Ryan Svenja[3]

[1] Helmholtz Centre for Polar and Marine Research, Alfred Wegener Institute, Bremerhaven, Germany; [2]Akvaplan-niva AS, High North Research Centre, Tromsø, Norway; [3] Helmholtz Centre for Polar and Marine Research, Alfred Wegener Institute, Bremerhaven, Germany

ABSTRACT

The Antarctic Slope Front (ASF) is important for limiting the Warm Deep Water (WDW) getting onto the continental shelf. The objective of this project is to study the seasonal inflow of this WDW into the continental shelf in the Filchner Rhone ice shelf and potentially the role of eddies on this inflow. Tree years (1989, 2009, and 2010) of daily output of Finite Element Sea-ice Ocean Model (FESOM) were used for this study. Five section were define: two on the coastal part and three far away from the coast in which we look at the Temperature, salinity, horizontal velocity, buoyancy frequency, vertical shear and Richardson number. The analyses based on the sections of temperature and salinity show that during the westward progression along the continental shelf, more WDW is getting into the continental shelf. However, there is more WDW on the shelf in summer than in winter. The resolution of model was not good to track eddies. Nevertheless, our hypothesis being that the intense eddy activity across the ASF play a potential role in the seasonal inflow of warm water onto the continental shelf, which is stronger in summer compared to winter, we then look at the background field by calculating the buoyancy frequency, vertical shear and Richardson numbed. The analyses show that the change from surface intensified shear in the narrow continental shelf to bottom intensified shear in the wide continental shelf is consistent with the dense outflow of WDW over the wide shelf region as opposed to the narrow shelf region.

Key points

- More WDW is getting into the continental shelf during the westward propagation
- WDW on the shelf is more in summer than in winter
- The change from surface shear to bottom shear is consistent with dense outflow of WDW over the wide shelf as opposed the narrow shelf.

1. Introduction

Glacial flow and sea level rise in the Antarctica has been attributed to the reduction of buttressing of ice sheet [*Dupont and Alley*, 2005], cause by the thinning of Antarctic ice shelves with an accelerating rate [*Paolo et al.*, 2015]. The cause of the ice shelf thinning is the enhancement of basal melt [*Pritchard et al.*, 2012] and is therefore linked to increase heat transport from the open ocean towards the ocean cavity beneath the ice shelves. [*Pritchard et al.*, 2012] show that this basalt melt is caused by increased flow of warm Circumpolar Deep Water (CDW) into the ice shelf cavities. [*Pritchard et al.*, 2012; *Paolo et al.*, 2015] found that Warm water open ocean origin has direct access to the ice shelf cavities in the west of the Antarctic Peninsula where the ice shelves are observed to be rapidly thinning. There is, therefore, a clear interest in studying the interaction between the ice shelves and the Southern Ocean from both the perspective of Antarctic glaciology and the change in sea level [*Nicholls et al.*, 2009].

The Filchner-Ronne Ice Shelf (FRIS) is the dominant glacial feature in the Weddell area and the second largest ice shelf after Ross Ice Shelf in the Antarctica [*Nicholls et al.*, 2009]. It float over the southern Weddell sea continental shelf and plays a major role in converting a sizable fraction of shelf water into a form that is able to flow into the deep sea [*Foldvik and Gammelsrød*, 1988; *Foldvik et al.*, 2004; *Nicholls et al.*, 2009]. In the southern Weddell Sea where is located the large FRIS, the water both on the wide continental shelf (separating the ice-shelf cavity from the deep ocean) and inside the ice shelf cavity is cold with temperatures being close to the freezing point (-1.9 C) [*Nicholls et al.*, 2009; *Orsi and Wiederwohl*, 2009]. The basalt melt rates observed on those regions are relatively low (~0.13m/yr) [*Rignot et al.*, 2013].

The Warm Deep Water (WDW) is originated from CDW which enter the Weddell Sea (WS) in the east and is carried westward in the southern part of the Weddell Gyre (WG). It is the key water mass of the Antarctic Circumpolar Current (ACC) [*Darelius et al.*, 2016; *Ryan et al.*, 2016]. Beside the solar radiation, WDW is the only source of heat for the WG [*Ryan et al.*, 2016]. The WDW is found from 300m depth in the interior of Weddell basin, below a cooled layer [*Darelius et al.*, 2016]. His temperature is between 0 – 1.5 ^{0}C. The WDW is separated from the shelf water (cool and fresh) by a front over the continental break usually called Antarctic Slope Front (ASF).

This front manifests through downward sloping isopycanls towards the continent along the narrow continental shelf break in eastern Weddell Sea with a V-shape structure over the continental slope of the Southern Weddell Sea [*Fahrbach et al.*, 1992]. The mixing along the pycnocline of the ASF creates a slightly cool and fresh water located just above the WDW and known as Modified Warm Deep Water (MWDW). The ASF is characterized by the southward depression of the WDW, isopycnals and Thermocline toward the continental slope [*Jacobs*, 1991]. This southward depression indicates a convergence of Ekman transport and down welling along the coast, driven by easterly winds along the Antarctic continent [*Dupont and Alley*, 2005; *Paolo et al.*, 2015]. Weaker summer winds caused both the shoaling of the thermocline and a seasonal inflow of WDW along the eastern flank of the Filchner Depression (FD) [*Darelius et al.*, 2016]. FD is a trough of 100km width that cross the eastern part of the wide continental shelf (600m depth sill) and extend until the south (1000m depth) in the FRIS cavity. This trough is filled with a dense water masse called Ice Shelf Water (ISW) with temperature close to the freezing point (<-1.9 C), which flows from the FRIS cavity to the sill with an estimated rate of 1.6 Sv [*Foldvik et al.*, 2004].

The ASF is important for limiting the WDW getting onto the continental shelf. However, recent sea-ice ocean model results [*Hellmer et al.*, 2012; *Timmermann and Hellmer*, 2013] suggest the changes in the slope current direction due to the modification of momentum transfer from atmosphere to ocean. These changes will allow the WDW to enter into the FRIS cavity trough the FD, thus increasing the basalt melt rates of this large ice shelf from 0.2 to 4m/yr within the next century [*Hellmer et al.*, 2012]. [*Gill*, 1973] demonstrated the association of the slope current to the coastal one in their westward propagation.

Figure 1 shows the study area. In the eastern part of the WS, the continental shelf is very narrow, and the slope current there coincide with the coastal current (dotted yellow arrow). The current during his westward propagation, bifurcates into a coastal current (dark yellow) and slope current (dotted yellow) at 27 ^{0}W where the continental shelf start to be wide. Below the bifurcation is the violet arrow that indicates the ISW flowing out of the FD to the sill.

Some models simulations investigate on the impact of flow instability of the slope current [*Dinniman et al.*, 2011], thermocline response to surface wind stress [*Hattermann et al.*, 2014] and mesoscale eddies [*Nøst et al.*, 2011; *Stewart and Thompson*, 2013] on the on-shore heat transport along the ASF. They could not provide a clear answer about the causes for the predicted circulation change in the FRIS. To provide an element of answer to this question, [*Daae et al.*, 2017] use a

High-resolution idealized models to investigate the change in the balance between the wind-driven Ekman overturning and a counteracting eddy overturning when changing from narrow to wide continental shelf through the FD. They found more warm water on the shelf (with the presence of fresh surface water) during summertime. This summer scenario is due to the partial balance of Ekman down welling by the shallower eddy overturning associated with the upper ocean stratification [*Daae et al.*, 2017]. Model studies [*Daae et al.*, 2017] suggest circulation change in which, warm water would access the shelf during wintertime. This predicted change is linked to the stratification during wintertime due to the weakening of convection by the reduction of sea ice production and the warmer and wetter atmosphere that will lead to the freshening of the upper atmosphere.

In this study, we hypothesize that the intense eddy activity across the ASF plays a potential role in the seasonal inflow of warm water onto the continental shelf, which is stronger in summer compared to winter. To justify our hypothesis, we investigate tree years (1989, 2009, and 2010) of daily output of Finite Element Sea-ice Ocean Model (FESOM) where we look at five sections (two in the narrow continental shelf and tree in the wide continental shelf, the sections are in red in the Figure 1. Part 2 shows the model description and the methods, part 3 shows the model results, part 4 shows the discussion of the results and model limitations and finally, the summary of the results are shown in part 5.

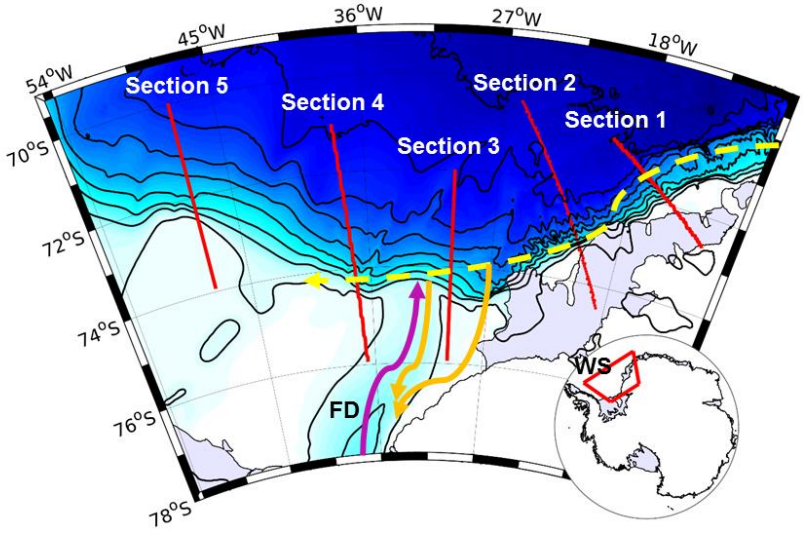

Figure 1. Southern Weddell Sea. Contour of the Bathymetry is shows every 500m. The five sections in red show the location of the section describe in the text. From right to left are section 1, section 2, section 3 section 4 and section 5. Ice shelves areas are shaded in light gray and while

color is land. The dotted yellow line is the slope current. Dark yellow arrows are the coastal current and the inflow through the FD and the violet arrow shows the outflow of ISW through the FD. The inset located at the bottom right shows the Antarctic continent, with the Weddell Sea (WS) shows in red contour.

2. Data and methods

2.1.Description of the model

The model used in this study is FESOM (Finite Element Sea-ice Ocean Model) developed at Alfred Wegener Institute (AWI) [*Timmermann et al.*, 2009], as an improvement of the Finite Element Ocean Model (FEOM) (Danilov et al., 2004). It was built from the Finite Element model of the North Atlantic (FENA) described by [*Danilov et al.*, 2005]. It solve the hydrostatic primitive equation based on an unstructured grid that consists of triangle at the surface of ocean and tetrahedral in the interior of the ocean [*Timmermann and Hellmer*, 2013].

The model use hybrid grid in the vertical with 22 sigma layers (terrain following) going from the continental shelf to 2500m depth (those sigma layers are used only around Antarctica) and 36 fixed layers (z coordinate) in the rest of the domain. The structure of these layers are shown in Figure 2.

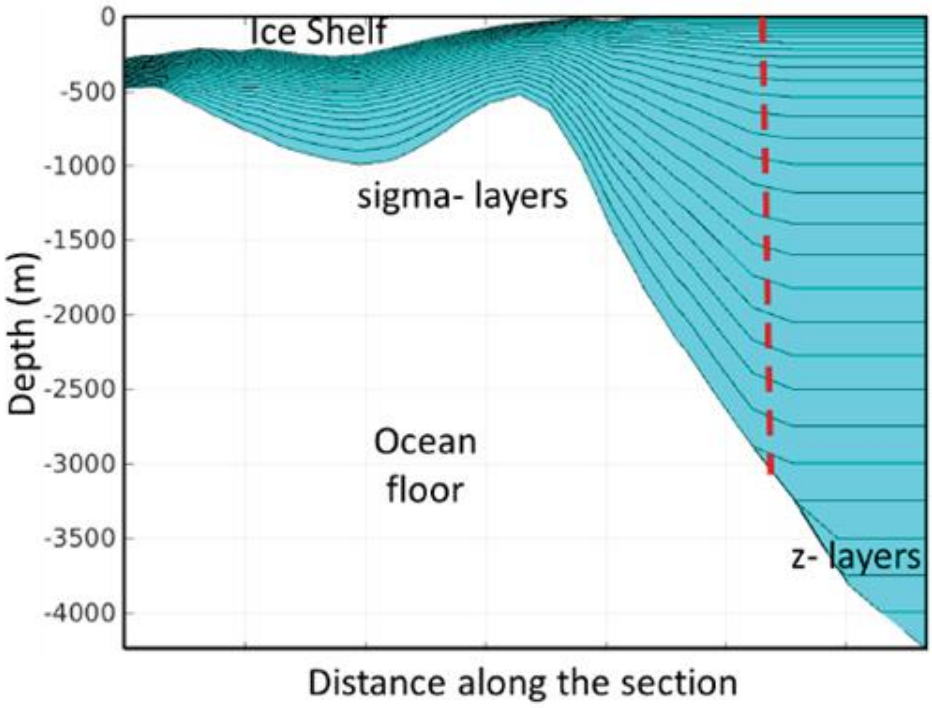

Figure 2. Distribution of the vertical layer around the Antarctica. On the left is represented the sigma layer under the ice shelf. They follow the bathymetry and extend up to almost 3000m depth.

On the right is the fixed layers (z coordinate). The dotted red vertical line is the transition between the sigma layers and the fixed one [*VanCaspel*, 2016].

FESOM is a fully coupled combination of oceanic to finite element model that includes ice shelf cavities and a dynamic-thermodynamic component of sea ice and has been proven as an important tool to study the Southern Ocean [*Timmermann and Hellmer*, 2013; *VanCaspel*, 2016]. The model describes the ice-shelf-ocean interaction, which impose a fixed sub ice shelf cavity geometry and thermodynamic coupling through the three system of equation proposed by [Hellmer and Olbers, 1989] to compute the temperature and salinity. The model is configured for a global domain with focus on the southern and western Weddell Sea where the horizontal model resolution (defined by surface node per unit of surface) is increased. It general configuration consists of a hybrid grid of 3 to 30 km for the southern ocean (Figure 3). In ice shelves especially under FRIS, the resolution increased. Outside of southern ocean, the resolution decrease considerably. For example, it has the resolution in the range of 250 – 300 km for the Atlantic and Pacific oceans [*Timmermann and Hellmer*, 2013].

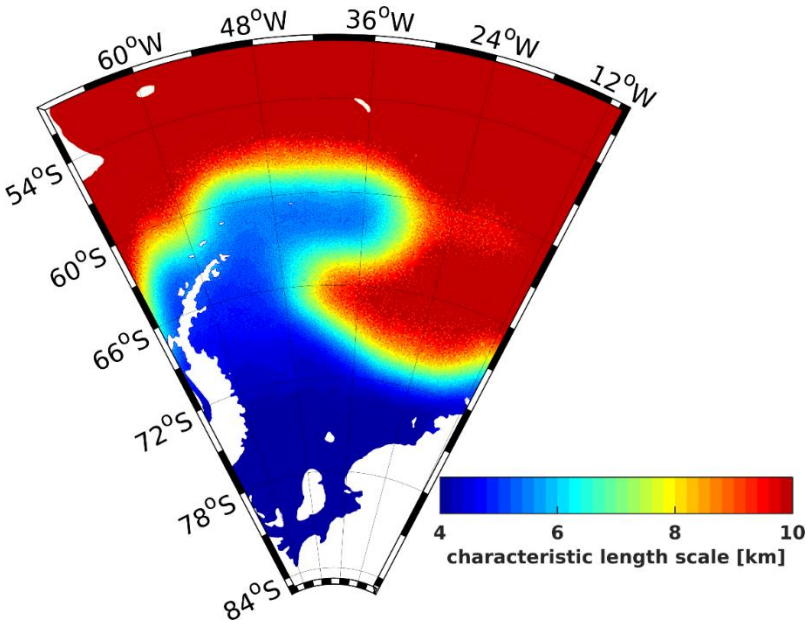

Figure 3. Grid length scale in southern part of the Weddell Sea.

RTopo-2 dataset has been used to prepare the bathymetry because of the fact that this dataset considers data from many of the most recent surveys of the Antarctic continental shelf

*[Timmermann and Hellm*er, 2013]. *[Timmermann an*d Hellmer, 2013] give more details about the bathymetry, ice shelf draft and cavity geometry.

FESOM simulations was initialized using the salinity and temperature fields from World Ocean Atlas 2013 [*Levitus et al.*, 2013]. The model is forced with the National Centers for Environmental Prediction Climate Forecast System Reanalysis (NCEP-CFSR, [*Saha et al.*, 2010]). (6-hour fields of air temperature, longwave and shortwave radiation, zonal and meridional wind, humidity, precipitation, and evaporation) [*VanCaspel*, 2016]. The model was run with monthly output for the period 1979-2010 and for three years (1989, 2009 and 2010), daily output was created. In this project, we are using those three years of daily output.

The aim of the project is to study the seasonal inflow of Warm Deep Water in the FRIS and to look at the background field to see the impact of eddies on this seasonal inflow. To achieve the goal of the project, temperature, salinity and horizontal velocity data are analyzed.

2.2.Observations data

To validate the model's ability to represent realistically the dynamics of the ocean, a comparison with observations is necessary.

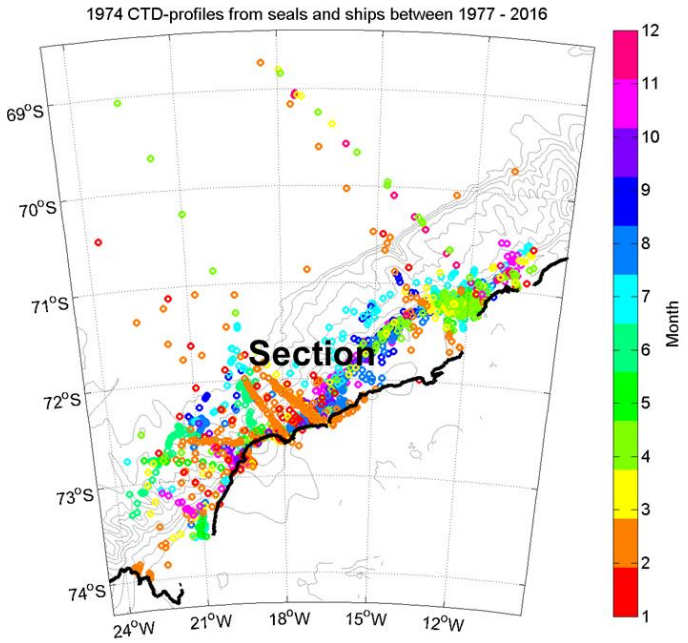

Figure 4. Monthly distribution of 1974 CTD profile collected from seals and ships between the

periods of 1977 to 2016. The word section indicates the position of the section created from the climatological mean *[Hattermann in prep.]*.

The observation data (Figure 4) are 1974 of Conductivity Temperature and Depth (CTD) profiles from seals and ship (Figure 4) collected in the period of 1977 to 2016. These data have been used to create a climatological mean section as follows *[Hattermann in prep.]*. Assuming that the ASF closely follows the continental shelf break topography, the individual profiles were sorted into depth classes based on the isobaths associated with the respective profile locations. A representative mean section was then constructed by averaging all profiles within each depth class after re-sampling on common z-levels. A monthly climatology was obtained by sorting the data into monthly time bins prior to the averaging. Finally, a combination of median and running mean filtering was applied to smoothen the fields along the time and space domain. For the validation of the model, the section 2 (Figure 1) of the FESOM simulation is compared to the define section in the observation

2.3. Methods

The daily data produced by FESOM are the unstructured one. For this project the data was resampled onto a structured grid. We started to use those structures daily data for applying eddy tracking algorithms created by [*Nencioli et al.*, 2010] , but found that the model was not capable of explicitly resolving the eddy (appendix 1 , Figure 1.1 is a daily field showing the features that are identified as eddies by the algorithm). We then decided to look at the background field by studying the buoyancy frequency, vertical shear and Richardson number in order to explain eddy activity and show which impact they have on the inflow of WDW on the continental shelf. The five sections defined in the Figure 1 are created from the climatological mean that we calculate using the structure daily data for the years 1989, 2009 and 2010. The potential temperature, salinity and vertical velocity were used as reference for the study.

The Richardson number is define as the ratio between the buoyancy frequency and the vertical shear. It help to investigate density and baroclinic current in the ocean.

$Ri = N^2/S^2$ Is the Richardson number where , $N = sqrt(\frac{g}{\rho 0}\frac{d\rho}{dz})$ Is the buoyancy frequency, which describe how the water is stratified and $S = sqrt(\left(\frac{du}{dz}\right)^2 + \left(\frac{dv}{dz}\right)^2)$ Is the vertical shear, which help to describe the baroclinicity of the current. g is the gravity ρ is the density, ρo is the

constant density (1027 kg/m^3 in this work), z is the depth, u, v are the vertical flow speed. When the Richardson number is big, the vertical shear is small, and then the water is more stratified, the inverse is also truth.

3. Results

3.1.Introduction of the study area

Figure 5 shows the bottom temperature (Figure 5a), bottom salinity (Figure 5b) and the bottom meridional velocity (Figure 5c). The red lines on the top are the location of sections 4 and 5 (from right to left). In the northern part is located the WDW. This water cross the shelf break where is located the slope current (Figure 5c) to enter the continental shelf at the eastern and western part of FD and especially where is located the section 4 and 5 and make change in the temperature and salinity. This southward propagation of the WDW is clearly specify by the meridional velocity (Figure 5c). Directly at the locations of sections 4 and 5, are the arrows which show this southward propagation.

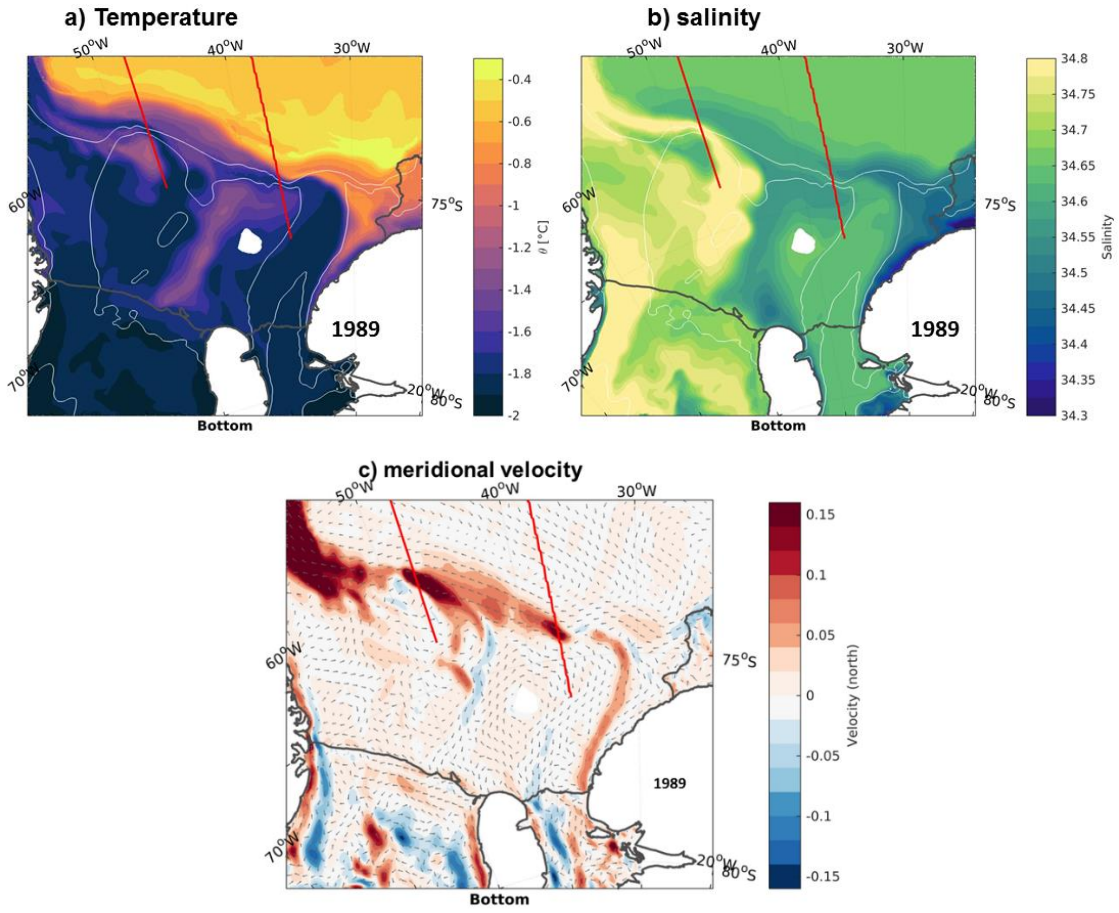

Figure 5. Bottom temperature (a), salinity (b) and meridional velocity (c) at the southern part of the Weddell Sea for the year 1989. The red lines are the location of the sections 4 and 5.

3.2.Model validation

The section 1 of model data (Figure 1) was chosen to be compared to the section define in the CTD profiles (Figure 4) for winter and summer.

Figure 6 is the comparison between the temperature, salinity in the model (Figure 6a, c) and the observation data (Figure 6b, d) in winter. The -0.5 °C isotherm (Figure 6a, b) is used to show the evolution of the thermocline and the 34.4 psu isohaline (Figure 6a, b) is used to show the location and evolution of the ASF. The model and data have the same pattern, cold and fresh water are observed in the surface and warm and saline water in the deep. Nevertheless, the mixed layer is deeper in the observation (Figure 6b) than the model (Figure 6a). The thermocline is narrow in the observation and wide in the model. It is found at the depth of 300m in the observation and 150m in the model at the open ocean and increase to more than 800m in the observation and 500m in the model near the continental shelf (Figure 6a, b). Below the Winter Water (WW), the WDW is found offshore from the depth of 300 m to 1000 m (Figure 6c, d), but with the only difference that the WDW is eroded in the model (Figure 6c). In the observation (Figure 6d), ASF is found at 200 m depth in the offshore and increased to 700m towards the continental shelf but in the model (Figure 6c), it is first wide and found at the depth of 100 m in the offshore and increased to 400m towards the continental shelf.

In summer (Figure7), Warm and fresh water is produced in a thin surface layer. The WDW core is less deep in summer than in winter, with the uplift of the isohaline 34.4 psu in summer. Still in summer, the thermocline is deeper and narrow in the observation (Figure 7a) than in the model (Figure 7b) and same thing for the ASF (Figure 7c, d).

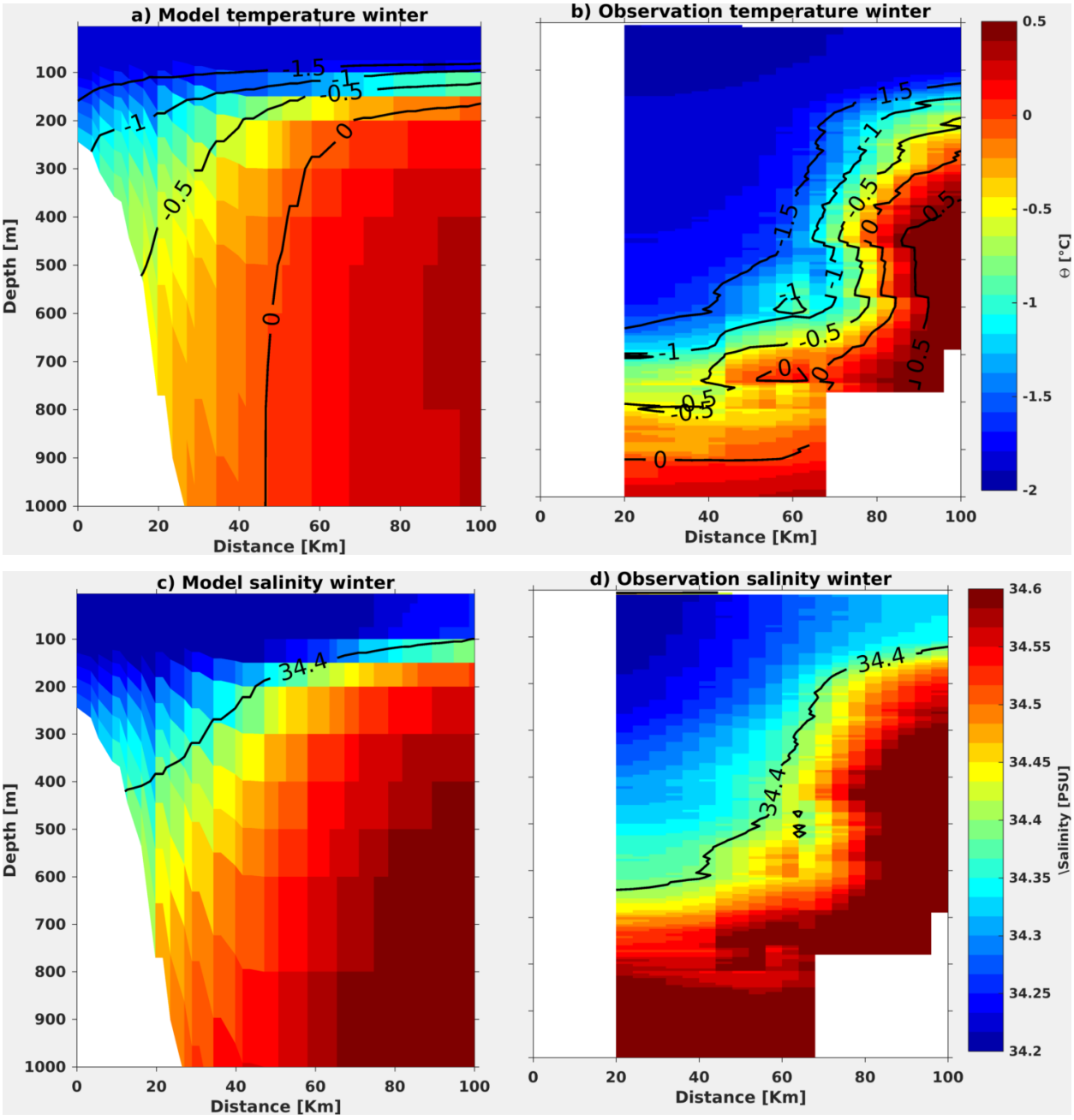

Figure 6. Temperature (a,b ; °C) and salinity (c, d ; Psu) for the model (left) and observation (right) in winter (June, July and August).

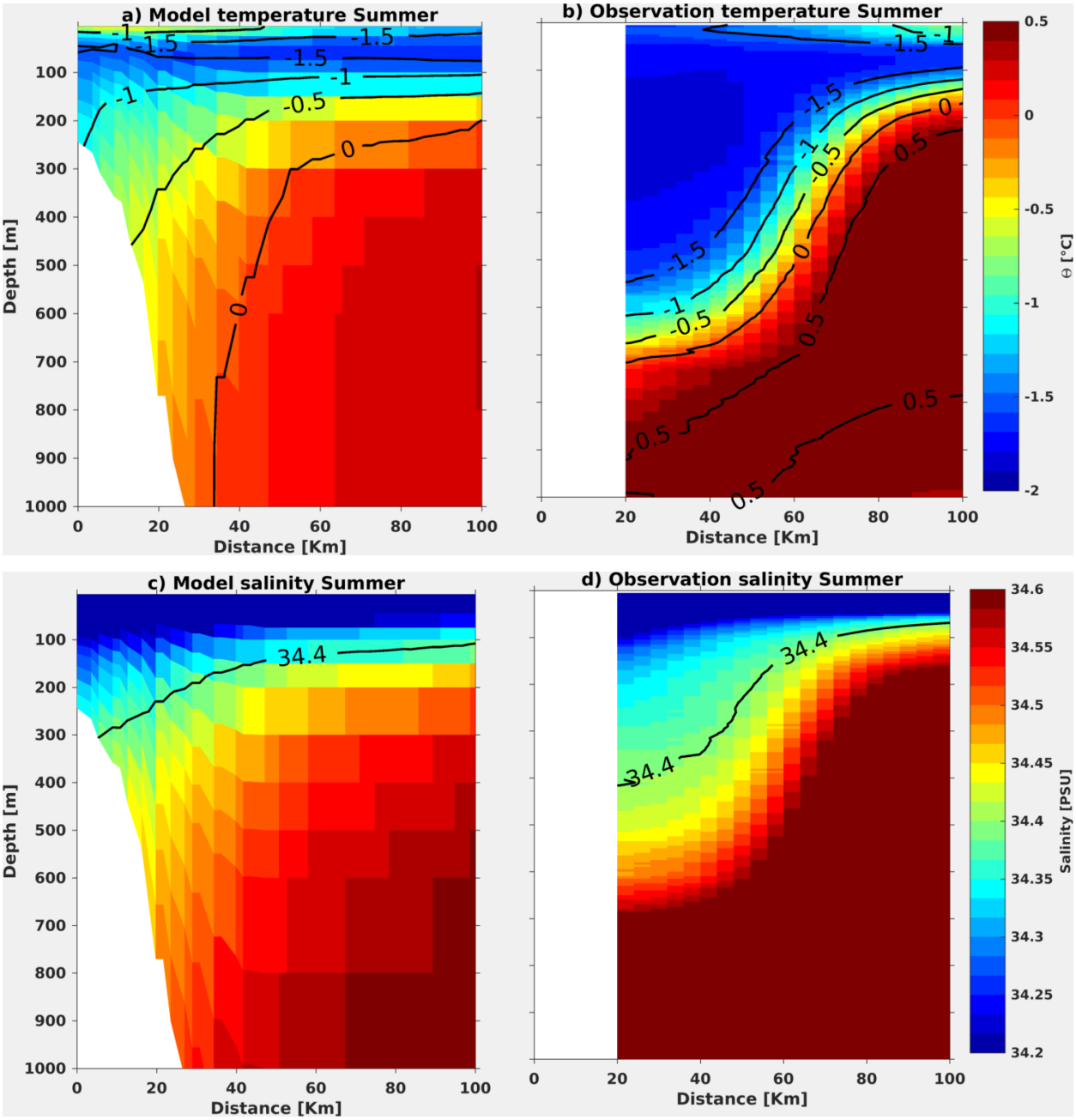

Figure 7. Temperature (a,b ; °C) and salinity (c, d ; Psu) for the model (left) and observation (right) in summer (January, February and March).

3.3.Description of water masses

Four water masses represented in the salinity temperature diagram (Figure 8) for section 1, section 2, section3, section 4 and section 5 (Figure 1), determine the temperature and salinity fields in the south-west of WS in summer (Figure 8, left) and winter (Figure 8, right). In summer, a warm and fresh water masse call Antarctic surface water (ASW) is produced in a thin surface layer by solar heating together with sea ice melt [*Hattermann et al.*, 2012]. During wintertime (Figure 8, right), the ASW change to WW, a homogeneous water mass with temperatures near the surface freezing point and salinities from 34.15 to 34.5 psu [*Nøst et al.*, 2011]. The ASF change its characteristic during the westward propagation along the continental shelf. The section 1, section 2 are located on the coastal part where the wind is weak in summer. This wind increases during the westward propagation [*Darelius et al.*, 2016] where is located the section 3, to 5 and creates some down welling effect. The obvious difference in ASW between the temperature and salinity reflects the spatial variability in consequence to vertical mixing due to the wind. The water masses found at western shelf in FRIS (present in Section 4 and 5) are higher in temperature and salinity than the WW. This water masse with temperature between -1.6 and 0.7 °C and salinity between 34.5 – 34.57 psu is known as Western Shelf Water (WSW). A straight line sloping between the WW (ASW) in winter (summer) and the WDW correspond to the MWDW, which has been transported on-shore. In addition, the straight line sloping from 34.3/-1.25 deg to 34.05/-2 deg in (section 1 and 2, circle with pink color) is a modified water coming from the mixing between the MWDW and the ISW and is homogenous in winter. This water is found only in the ice self-cavity where flow the coastal current (Figure 9c).

3.4.Description of temperature, salinity and vertical velocity in the shelf break

In this part we are looking at the section plot of temperature, salinity and horizontal velocity in the section 1 located in the narrow continental shelf and section 4 in the wide part (Figure 1) to explain the behavior of the WDW towards the continental slope during the westward propagation. Figure 9 shows the section 1 in winter (top) and summer (bottom). The surface water is very cold (around 1.9 deg Figure 9a, top).

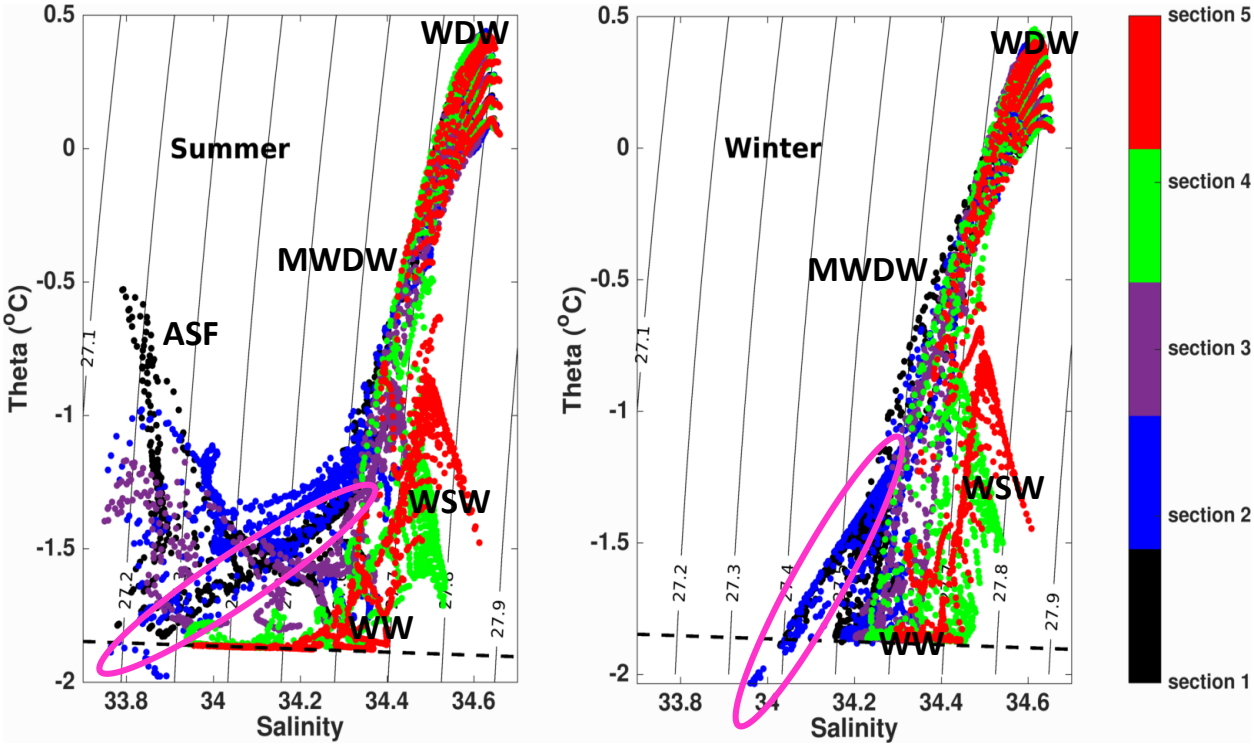

Figure 8. T–S diagram in (left) summer and (right) winter for the five sections combines. The dashed line at -1.9 °C indicates the freezing point.

A clear structure of WDW is see under the thermocline (Figure 9a, top), which separate that water from the cold one located in the upper ocean. The thermocline is found at the depth of 150m at the open ocean and increase to more than 500m near the continental shelf (Figure 9a, top). The WW- layer extent over the continental slope to a depth more than 600m (Figure 9b, top). ASF is found at 200 m depth in the offshore and increased to more than 600m towards the continental shelf (Figure 9b, top). In summertime (Figure 9, bottom), the water is warm and fresh in the surface layer (Figure 9a, b, bottom). The fresh water is coming from the ice melt. The isohaline is uplift in the continental slope (from more than 400m in wintertime to 300m in summertime). The horizontal velocity in winter (Figure 9c, top) shows that the presence of the slope front that separates the WDW core from the coast seems to be located far away from the coast where is located a strong current very wide and deep (around 80-180 Km of distance and 5-1000m of depth). This strong current is associated with the WW and contribute to deepen the isohaline at the continental slope. Thus preventing the WDW to reach the continental shelf. A second current call coastal current, which is totally separated from the current associated with the ASF is present

(Figure 9c, top). This current flow southward in the ice shelf cavity. It help for the mixing of ISW (cold and fresh water, Figure 9a, b, top) and the MWDW that reach the continental shelf. In summertime, the current associated with the ASF become weak and divides into two part (Figure 9c, bottom). One part is located in the offshore and the other part approaches the coastal current on their westward progression. This explain the fact that the coastal current is stronger in summer than winter. The inflow of MWDW and ASW in the ice shelf cavity as see in the temperature and salinity are clearly reflected by this westward propagation in summertime. The reduction of the slope current intensity in summertime explains the uplift of isohaline 34 psu during this period.

The section 4 (Figure 10) is located far away from the coast and ice shelf. This is explained by the absence of coastal current. The isohaline 34.4 psu is lifted above the continent slope and reach the continental shelf (Figure 10b, top). Slightly offshore of the shelf edge, is observed a doming of the thermocline (Figure 10a, top) between the WDW and WW. This doming indicates the upwelling events [*Fahrbach et al.*, 1994], which explains the presence of WDW, on the continental shelf (Figure 10b, top). Since the section cross the shelf break, we have the presence of slope current associated with the ASF. However, this current is less strong and less deep than the one found in the section 1. This slope current combine to the upwelling event, explain the presence of the V-shape front (Figure 10b), represented by the isohaline 34.4 psu. In summertime, the slope current (Figure 10c, bottom) become weaker and then contribute to the uplift of V-shape (Figure 10b, bottom) and more WDW on the continental shelf. The maximum depth of the isohaline is about 300m (Figure 10b, top) in wintertime, while it is about 170m in summertime (Figure 10b, bottom).

Figure 11 shows the time series of the maximum depth of 34.4 psu isohaline along the continental slope for the sections 1 to 5 (Figure 1). The five sections show the similar patterns with larger special and temporal variability. The maximum depth from October to March is small compare to the one from April to September. The seasonality become weaker from section 1 to section 5. Below we will show that this special and temporal variability is due to eddies activities.

Figure 12 also shows the time series of the maximum depth of -0.5 °C isotherm of temperature. During the year, the thermocline vary a lot from time to time. The maximum depth of thermocline in the section 1 shows three seasonality. From November to March it reduces until the depth of 400m, then from march to July, it increases till the depth of about 600m and finally from July to November it decreases again until 500 m depth. At the section 2, a clear seasonality

between winter and summer is observed (high value in winter and inverse in summer). The section 3 is not clear some period in summer as for example January is found the maximum depth of thermocline and some period in wintertime as May is found the smallest value. The section 4 shows a clear seasonality as section 2. Finally, in the section 5 things flip up. The smallest value are in wintertime and the inverse in summer.

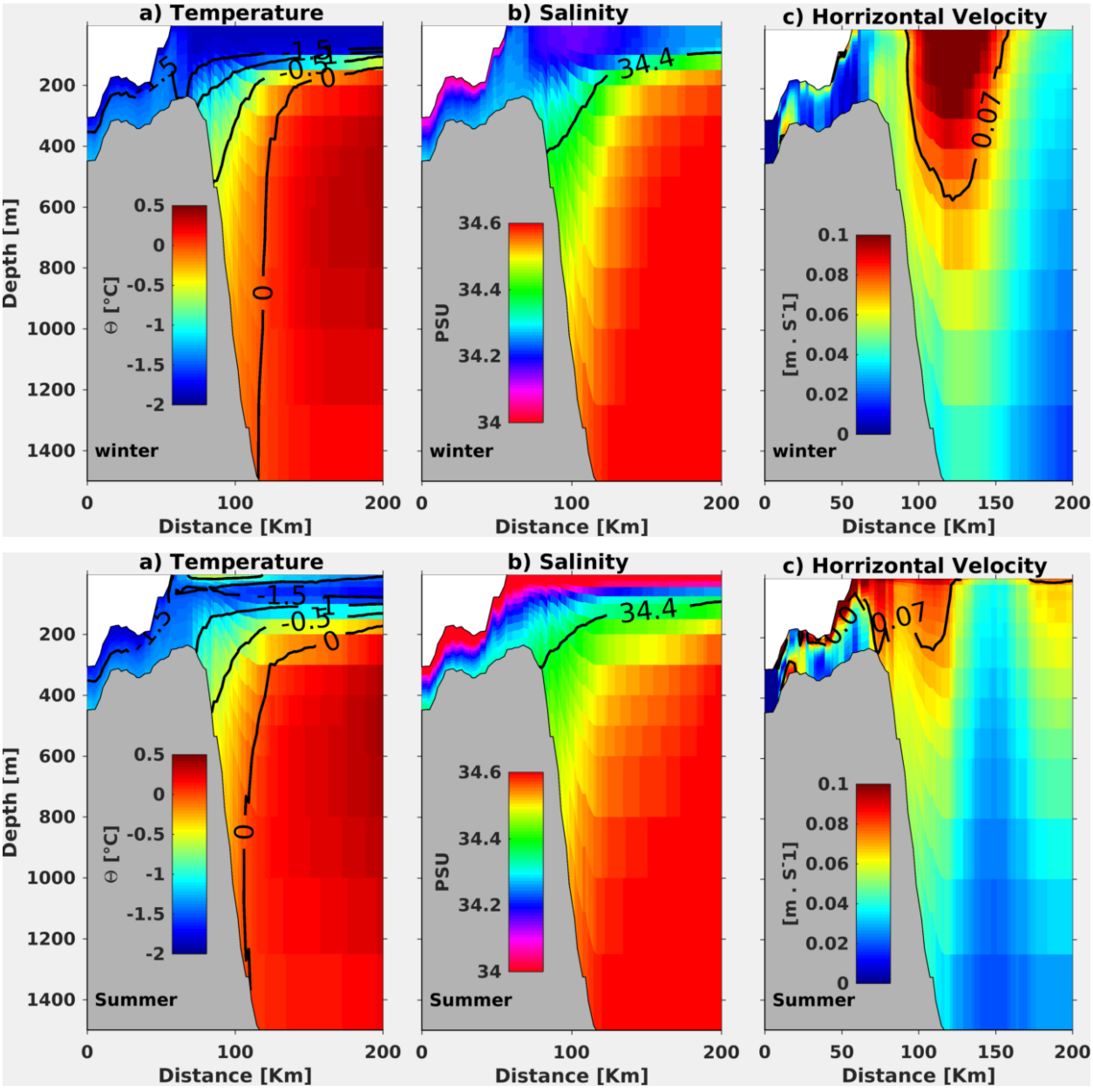

Figure 9. Section 1: Average of temperature, salinity and horizontal velocity (up) in winter (June/July/August) and (down) in summer (January/February/March). The isolines 34.4psu and 0.5 °C show the seasonal variability of the ASF.

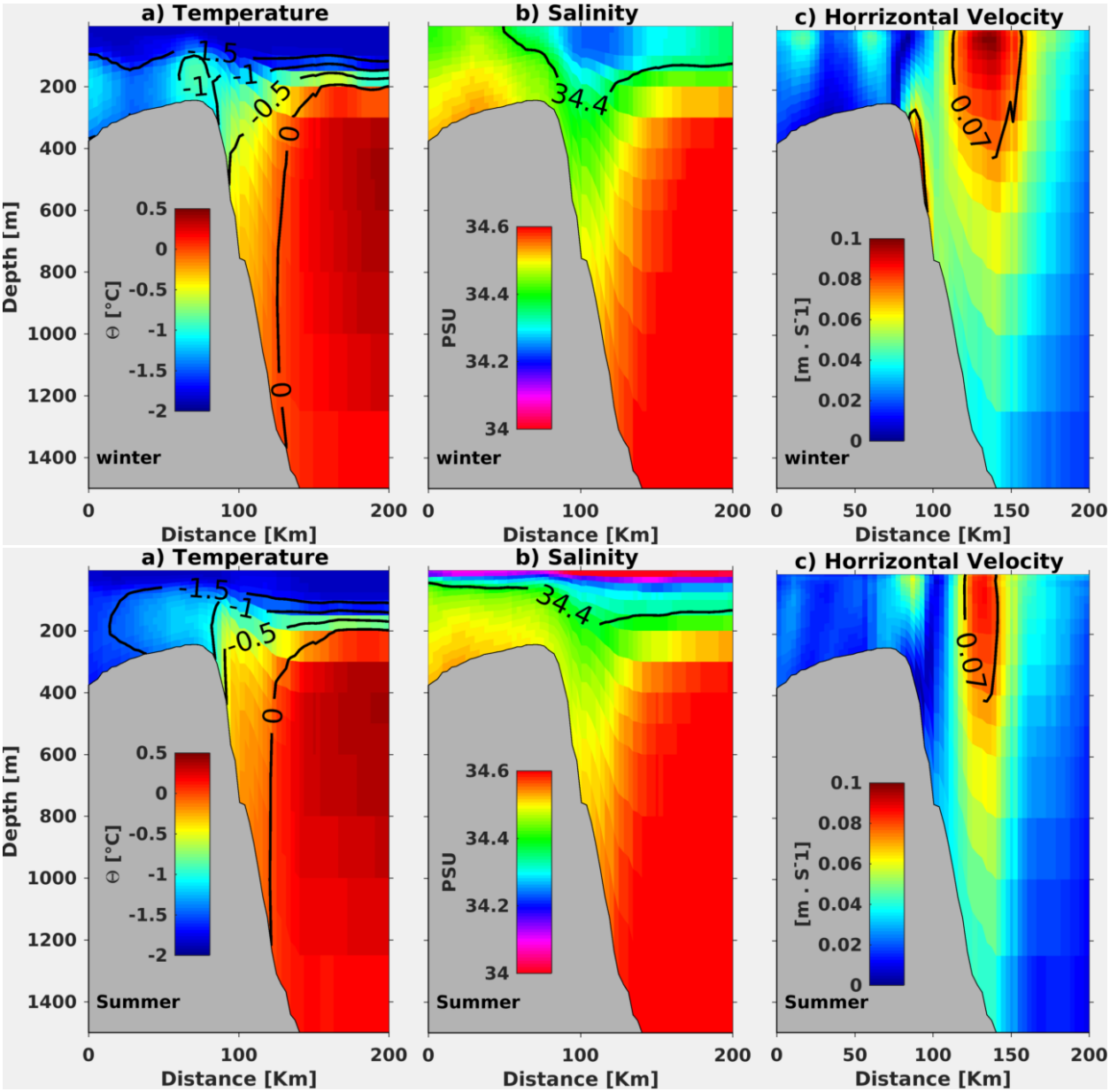

Figure 10. Section 4: Average of temperature, salinity and horizontal velocity (up) in winter (June/July/August) and (down) in summer (January/February/March). The isolines 34.4psu and 0.5 °C show the seasonal variability of the ASF.

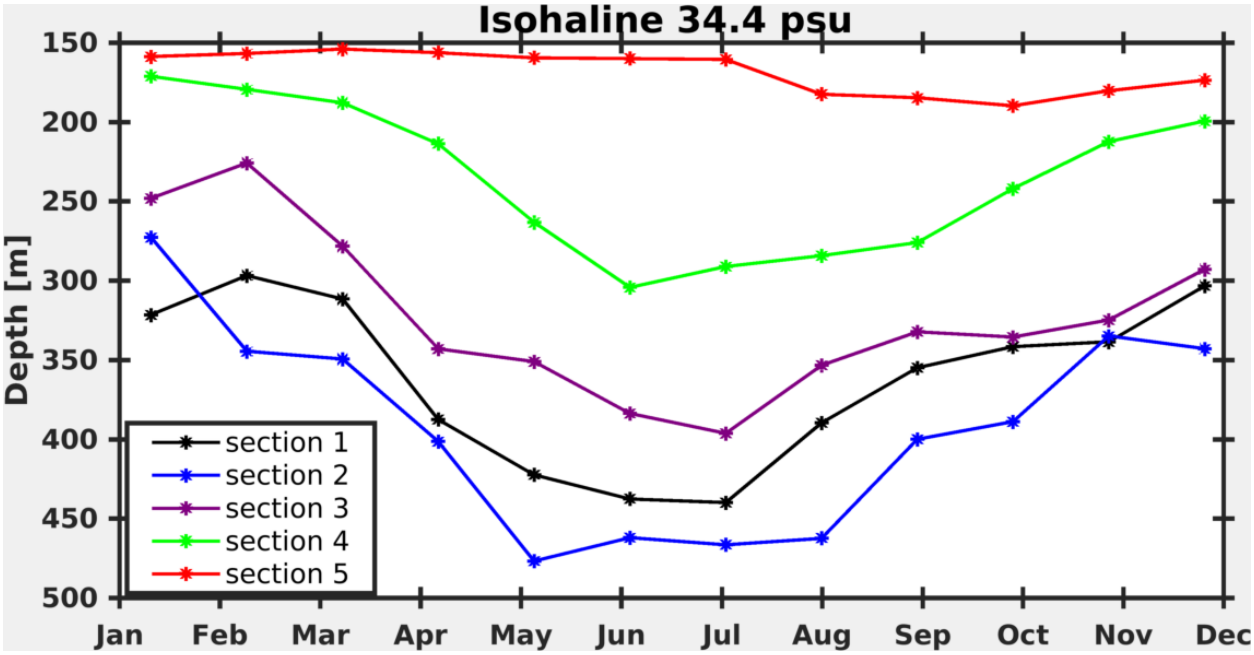

Figure 11. Time series of the maximum depth of isohaline 34.4 psu. The location of the sections is in the Figure 1.

3.5.Buoyancy frequency, vertical shear and Richardson number

In this part we are looking at the background field by study the buoyancy frequency, vertical shear, and Richardson number in order to explains the eddies activity and show which impact they have on the inflow of WDM into the continental shelf. The same section as described before are studied.

Figure 13 shows the section1 in winter (top) and summer (bottom). During the wintertime, stability N^2 (Figure 13a, top) is uniform and small in the first 100m. It start to increase markedly under the ice shelf where is flowed the coastal current (Figure 9c) and between 100-400 m depth from the continental slope to the offshore part.

The vertical shear (Figure 13b, top) is big from the surface offshore until about 900m depth of the shelf break. Nevertheless, immediately at the shelf break is found low value of vertical shear where the deepening of isohaline 34.4 psu is located. Under the ice shelf, from where is flowing the coastal current is found a big value of vertical shear. The Richardson number (Figure 13c, top) is the opposite of the vertical shear. The section plot of Richardson number shows a small number in the first 100m depth and under the ice shelf, a high number at the shelf break, a low value from

surface to 900m of depth immediately after the shelf break and again high value at the offshore part.

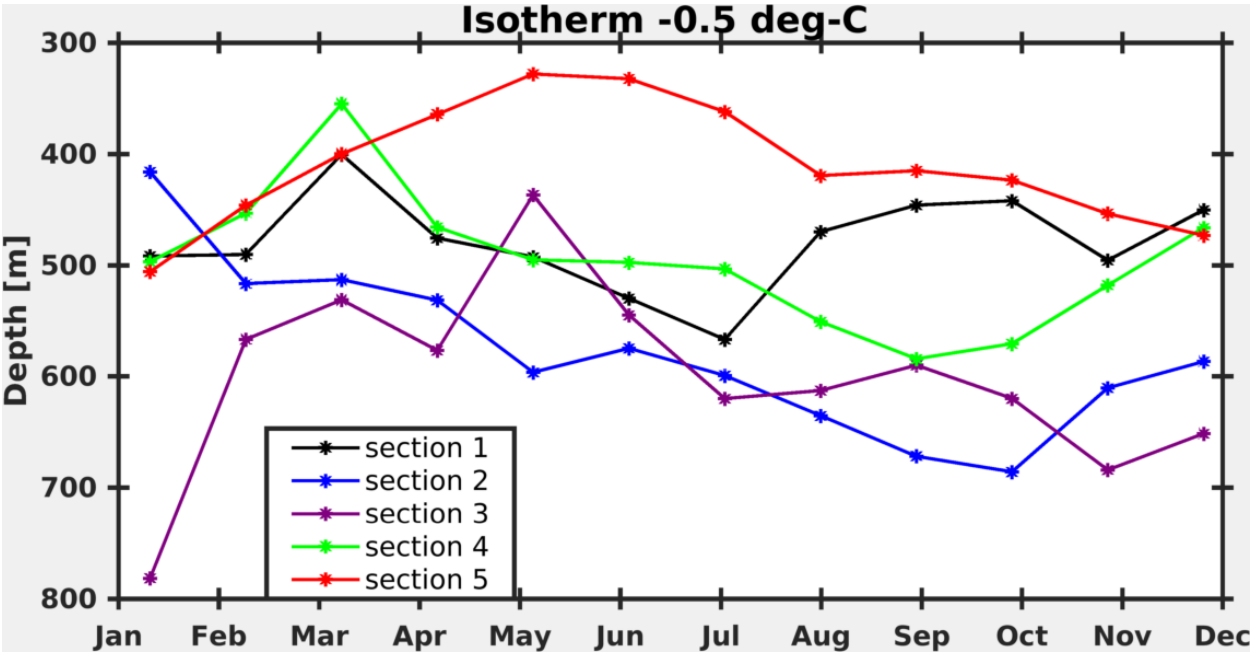

Figure 12. Time series of the maximum depth of isotherm -0.5 °C. The location of the sections is in the Figure 1.

In the summertime, the stability (Figure 13a, bottom) became very high at the surface until 400m depth in response to the meteorological condition and warming of the surface water. At the shelf break, under the ice shelf and at the surface, the vertical shear (Figure 13b, bottom) become more high compare to the wintertime, as expected. Meaning that there are some turbulence going on at the continental slope during this period and it can explain the uplift of the isohaline 34.4 psu (Figure 13b, bottom). The opposite is observed for the Richardson number. Nevertheless, the Richardson number is high at the surface compare to wintertime. This is due to the high stability.

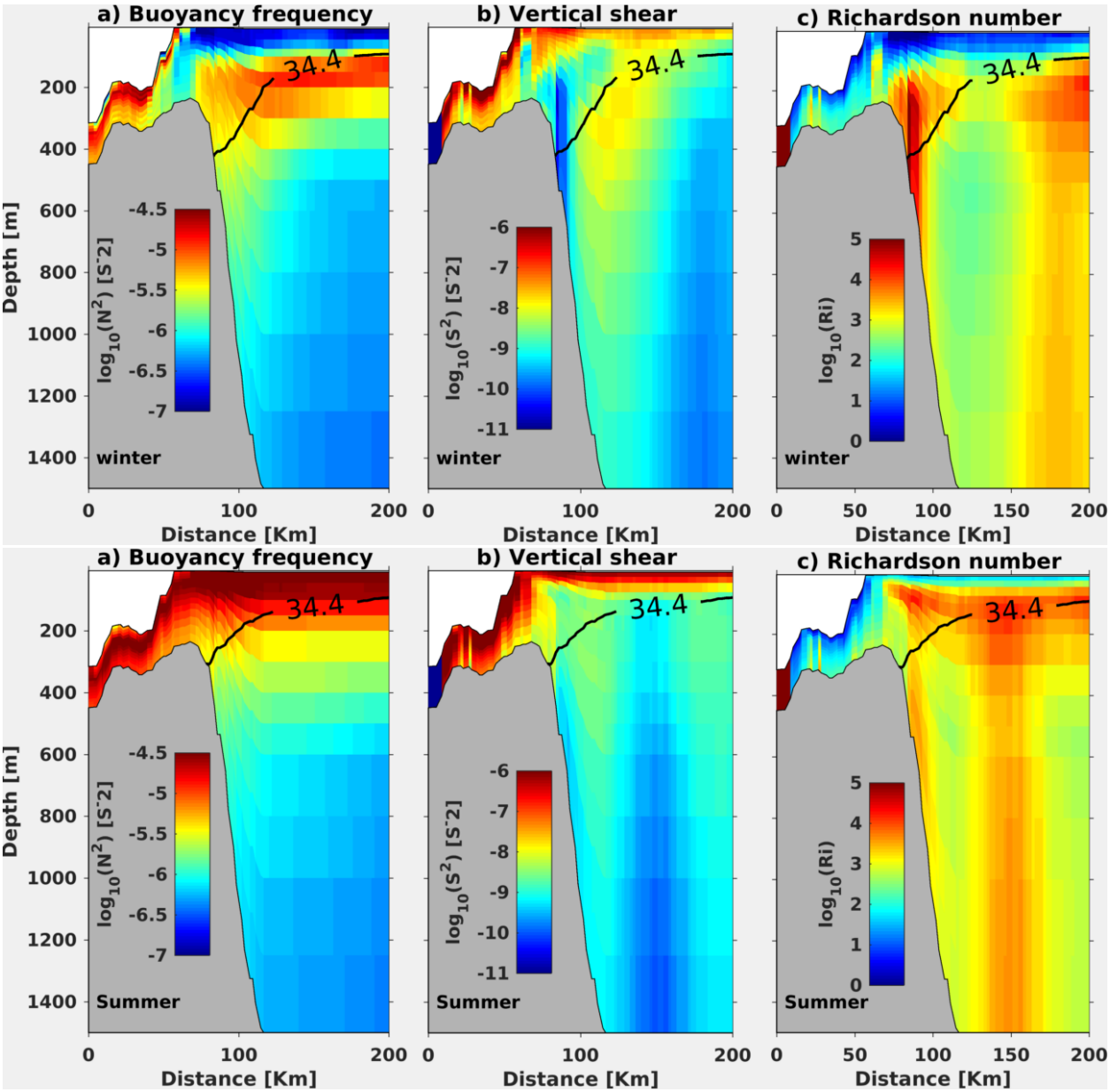

Figure 13. Section 1: Average of buoyancy frequency, vertical shear and Richardson number (up) in winter (June/July/August) and (down) in summer (January/February/March). The isohaline 34.4psu shows the seasonal variability of the ASF.

The section 4 (Figure 14) shows low stability in winter (Figure 14a, top) for the first 100m depth. From 100 to 400m depth, the stability start to increase, but by comparing to the section 1 it is small. The vertical shear (Figure 14b, top) is small at the surface compare to the section 1. The high value of vertical shear is observed directly at the shelf break and a bit far away of the shelf

break at the middepth. High value of vertical shear is observed on the continental shelf where we have the upward of isohaline 34.4 psu, which can be assimilate to the strong isopycnal slope on the continental shelf. Immediately after the shelf break is observed a low value of vertical shear. The Richardson number (Figure 14c, top) is the inverse of vertical shear. During the summertime, the stability (Figure 14a, bottom) became high at the surface due to the warming of the surface water, but still it is small compared to the section 1. The vertical shear (Figure 14b, bottom) decrease at the surface and on the continent shelf compare to the wintertime. The low value of the shear observed immediately after shelf break during wintertime, became weaker in summertime. The high value of shear at the shelf break and on the continental shelf is small compare to the wintertime. This is reflected on the downward of isohaline 34.4 psu on the continental shelf during summertime compare to the wintertime. In addition, between 300 – 1200m depth and 120-130km of distance is observed high value of vertical shear. The Richardson number varies opposite to the vertical shear. The same pattern or variation was noticed for the sections (section 3 and 5 that we did not show here) located in the wide continental shelf. In those sections, the isohaline 34.4 is above the continental shelf (Figure 10) and the WDW can reach there in every season but more in summertime.

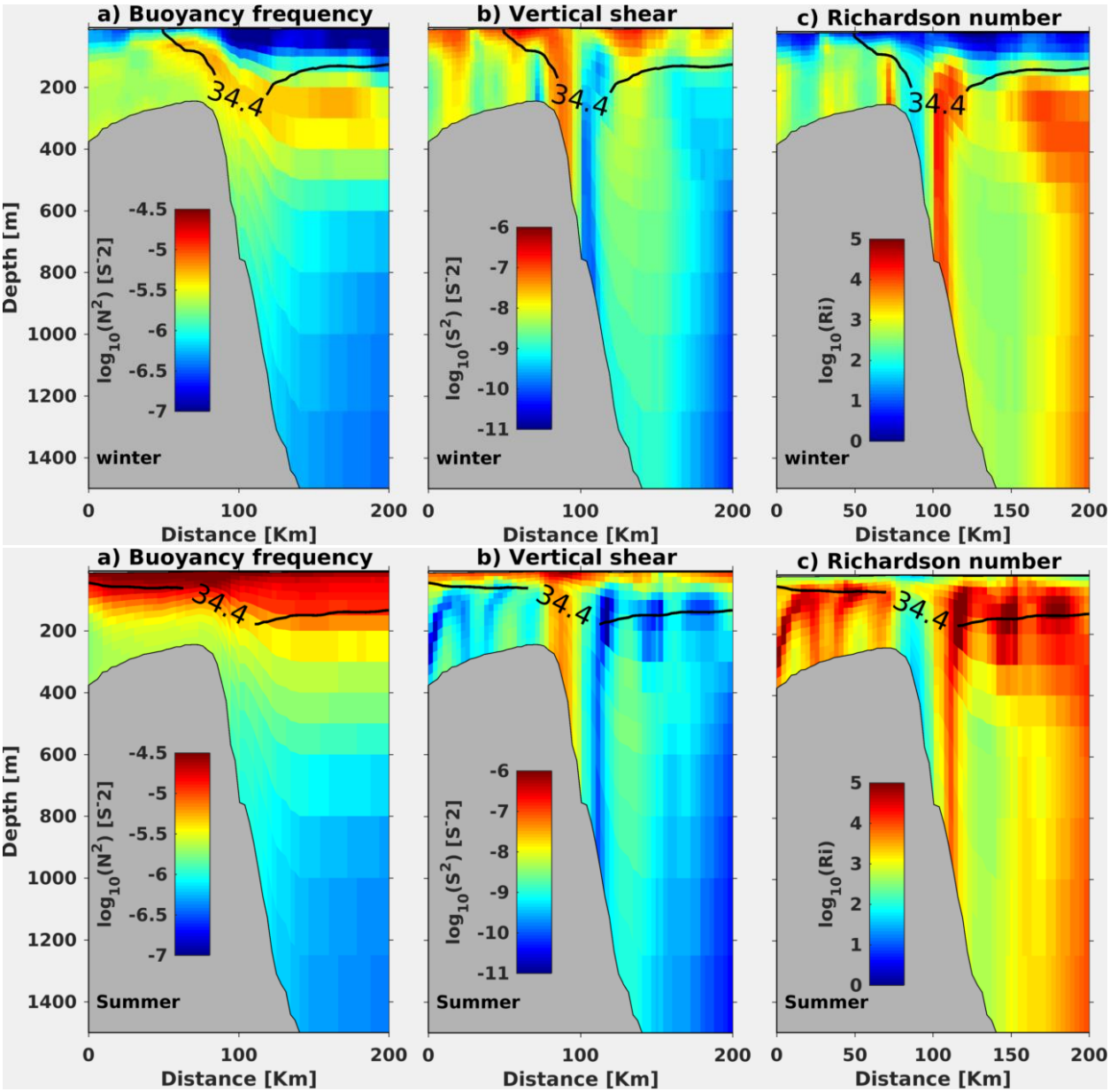

Figure 14. Section 4: Average of buoyancy frequency, vertical shear and Richardson number (up) in winter (June/July/August) and (down) in summer (January/February/March). The isohaline 34.4psu shows the seasonal variability of the ASF.

4. Discussion

Based on the FESOM monthly mean for the years 1989, 2009 and 2010, we look at the seasonal inflow of WDW into the continental shelf and potentially the role of eddies on this inflow. Our focus was FRIS. The processes that interact to control the access of WDW to the continental

shelf has been identified by comparing five different sections (Figure 1) (two in the narrow continental shelf and three in the wide continental shelf).

The analyses based on the section plot of temperature and salinity show that during the westward progression along the continental shelf, more WDW is getting into the continental shelf. This inflow is more in summertime than the wintertime. This is consistent with [*Årthun et al.*, 2012] who found from the moored instruments on the Weddell Sea shelf that warm inflow occurs during the summer season when the thermocline depth is shallower than during winter. The depth of thermocline close to the continental slope change from about 500m to 400m depth between winter and summer in the narrow continental shelf. This result march with the one found by [*Semper and Darelius*, 2017]. They found changes in thermocline depth about 200 m between winter and summer, at the Filchner sill. By looking at the Richardson number and vertical shear, we found that the upward of ASF in summertime is due to eddies activities. This is consistent with the result of [*Daae et al.*, 2017] who found that the increased southward transport of WDW during summertime is linked to a dynamic response, rather than to changes in the depth of the thermocline. In the wide continental shelf, the dense WW is transported offshore where the intensity of slope current is high. This explains the creation of V-shape structure across the continental slope. The change from surface intensified shear in section 1 to bottom intensified shear in section 4 is consistent with the dense outflow of WDW over the wide shelf region (Figure 5) as opposed to the narrow shelf region. This result agree with [*Stewart and Thompson*, 2016], who find that a pathway for CDW to access the continental shelf without doing work against the buoyancy force is created by an establishment of an isopycnal connection between the dense shelf water and the CDW.

During the westward propagation, we plot the time series of the maximum depth of isohaline 34.4 psu. We found that at the narrow continental shelf, the isohaline was deep in winter and shallow in summer but could not reach the continental shelf. On the wide continental shelf, the isohaline with a structure of V-shape could reach the continental shelf in every season but in summertime, it was upward compare to the wintertime. This result agree with [*Daae et al.*, 2017] who find found that eddy-mediated transport of WDW to the wide continental shelf is most efficient when dense water on the shelf is transported offshore, creating V-shaped structure across the continental slope.

The sections on the narrow continental shelf show the presence of two current: the slope current and the coastal current. They are both separated in winter and are associated together in

summer in their westward propagation. We found that the coastal current is associated with the fresh water and that it is strong in summertime compare to wintertime. This result agree with [*Graham et al.*, 2013] who found that the coastal current is likely to provide refresh signals located along the coast. This coastal current help for the mixing of MWDW and ISW under the ice shelf. Hence the creation of this straight line observed in the TS-diagram (Figure 8, circled with a pink color). During the wintertime, the slope current is associated with WW and contributes to deepen the thermocline and ASF below the shelf break. This current reduce considerably during the summertime. This reduction contribute to the upward of ASF and thermocline at the continental slope. In this study, we could not investigate on the causes of the slope current. Nevertheless our result is consistent with [*Darelius et al.*, 2016] who found that the depression of WDW and thermocline along the coast is due to the easterly winds along the Antarctic continent, which cause the convergence of Ekman transport and down welling along the coast.

During our study, we encounter some limitation with the model. The plan at the beginning was to track the eddy with and tracking algorithm, but because of the model resolution, we could not find enough eddy to highlight our hypothesis. We then jump into the background field where we could explain that even if our model could not reproduce enough eddy, still there is eddy activity on the shelf break, which play a potential role on the inflow of WDW into to the FRIS. We think that it will be important to make the same study with eddy, by using a tracking method where the composite of eddy can be done with temperature and salinity field, in order to see not only the contribution of eddy in general but the contribution of each type of eddy (anticyclonic and cyclonic eddy).

Conclusion

By using three years (1989, 2009 and 2010) of monthly mean of FESOM model, we investigate on the seasonal inflow of Warm Deep Water (WDW) in the Filchner Ronne Ice Shelf (FRIS). We find that during the westward progression along the continental shelf, more WDW is getting into the continental shelf and that this inflow is more in summertime than wintertime. The change from surface intensified shear in the narrow continental shelf to bottom intensified shear in the wide continental shelf is consistent with the dense outflow of WDW over the wide shelf region as opposed to the narrow shelf region.

Acknowledgements

The study was conducted as a part of Nippon Foundation- Partnership for Observation of the Global Oceans (NF-POGO) Centre of Excellence training program at Helmholtz Centre for Polar and Marine Research, Alfred Wegener Institute, Bremerhaven, Germany.

Appendix 1: Eddy tracking in the eastern part of the southern west of WS.

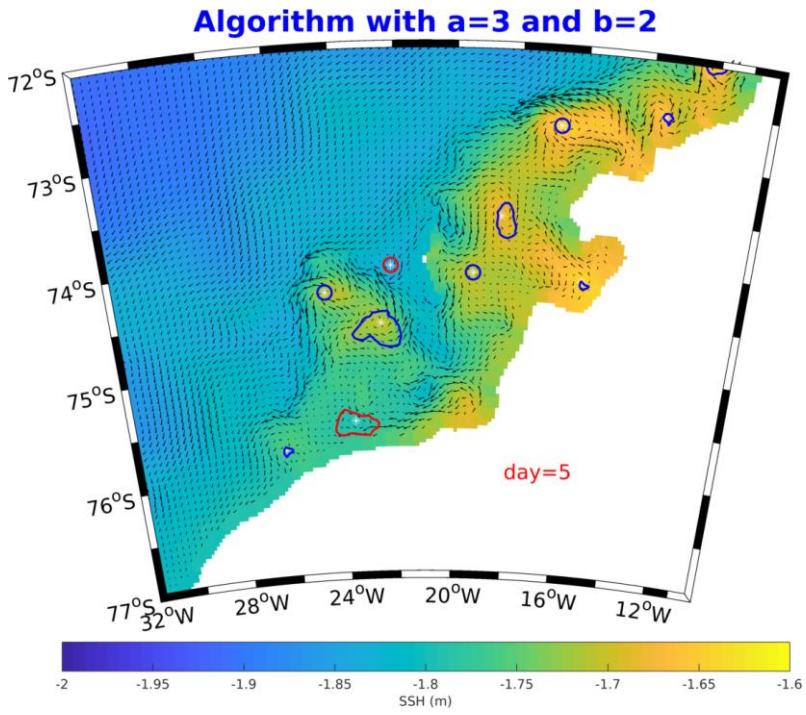

Figure 1.1 Map of the Sea Surface High (SSH) with the horizontal velocity on the top in the year 1989, day 5. The red contours is the cyclonic eddies and blue contours is the anticyclonic eddies. The parameter a help to determine the area of eddy and the parameter b help to detect the center of eddy. This algorithm is built on four constraints.

References

Årthun, M., K. W. Nicholls, K. Makinson, M. A. Fedak, and L. Boehme (2012), Seasonal inflow

of warm water onto the southern Weddell Sea continental shelf, Antarctica, *Geophys. Res. Lett.*, *39*(17), 2–7, doi:10.1029/2012GL052856.

Daae, K., T. Hattermann, E. Darelius, and I. Fer (2017), On the effect of topography and wind on warmwater inflow—An idealized study of the southern Weddell Sea continental shelf system, *J. Geophys. Res. Ocean.*, 2017–2033, doi:10.1002/2013JC009262.Received.

Danilov, S., G. Kivman, and J. Schröter (2005), Evaluation of an eddy-permitting finite-element ocean model in the North Atlantic, *Ocean Model.*, *10*(1–2 SPEC. ISS.), 35–49, doi:10.1016/j.ocemod.2004.07.006.

Darelius, E., I. Fer, and K. W. Nicholls (2016), Observed vulnerability of Filchner-Ronne Ice Shelf to wind-driven inflow of warm deep water, *Nat. Commun.*, *7*, 12300, doi:10.1038/ncomms12300.

Dinniman, M. S., J. M. Klinck, and W. O. Smith Jr. (2011), A model study of Circumpolar Deep Water on the West Antarctic Peninsula and Ross Sea continental shelves, *Deep Sea Res. Part II Top. Stud. Oceanogr.*, *58*(13–16), 1508–1523, doi:10.1016/j.dsr2.2010.11.013.

Dupont, T. K., and R. B. Alley (2005), Assessment of the importance of ice-shelf buttressing to ice-sheet flow, *Geophys. Res. Lett.*, *32*(4), 1–4, doi:10.1029/2004GL022024.

Fahrbach, E., G. Rohardt, and G. Krause (1992), The Antarctic coastal current in the southeastern Wedell Sea, *Polar Biol.*, *12*, 171–182.

Fahrbach, E., R. G. Peterson, G. Rohardt, P. Schlosser, and R. Bayer (1994), Suppression of bottom water formation in the southeastern Weddell sea, *Deep. Res. Part I*, *41*(2), 389–411, doi:10.1016/0967-0637(94)90010-8.

Foldvik, A., and T. Gammelsrød (1988), Notes on {S}outhern-{O}cean {H}ydrography, {S}ea-{I}ce And {B}ottom {W}ater {F}ormation, *Palaeogeogr. Palaeoclimatol. Palaeo-ecology*, *67*(1–2), 3–17.

Foldvik, A. et al. (2004), Ice shelf water overflow and bottom water formation in the southern Weddell Sea, *J. Geophys. Res.*, *109*(C02015), doi:10.1029/2003JC002008, doi:10.1029/2003JC002008.

Gill, A. E. (1973), Circulation and bottom water production in the Weddell Sea, *Deep. Res. Oceanogr. Abstr.*, *20*(2), 111–140, doi:10.1016/0011-7471(73)90048-X.

Graham, J. A., K. J. Heywood, C. P. Chavanne, and P. R. Holland (2013), Seasonal variability of water masses and transport on the Antarctic continental shelf and slope in the southeastern

Weddell Sea, *J. Geophys. Res. Ocean.*, *118*(4), 2201–2214, doi:10.1002/jgrc.20174.

Hattermann, T. (in prep.), Seasonal variability on the thermocline depth at the Weddell Sea continental shelf break – data synopsis and a simple model; Hattermann (2016); Conference presentation, 31st Forum for Research into Ice Shelf Processes, Gothenburg

Hattermann, T., O. A. Nst, J. M. Lilly, and L. H. Smedsrud (2012), Two years of oceanic observations below the Fimbul Ice Shelf, Antarctica, *Geophys. Res. Lett.*, *39*(12), 1–6, doi:10.1029/2012GL051012.

Hattermann, T., L. H. Smedsrud, O. A. Nøst, J. M. Lilly, and B. K. Galton-Fenzi (2014), Eddy-resolving simulations of the Fimbul Ice Shelf cavity circulation: Basal melting and exchange with open ocean, *Ocean Model.*, *82*, 28–44, doi:10.1016/j.ocemod.2014.07.004.

Hellmer, H. H., F. Kauker, R. Timmermann, J. Determann, and J. Rae (2012), Twenty-first-century warming of a large Antarctic ice-shelf cavity by a redirected coastal current, *Nature*, *485*(7397), 225–228, doi:10.1038/nature11064.

Hellmer, H. H. H., and D. J. J. Olbers (1989), A two-dimensional model for the thermohaline circulation under an ice shelf, *Antarct. Sci.*, *1*(4), 325–336, doi:10.1017/S0954102089000490.

Jacobs, S. S. (1991), On the nature and significance of the Antarctic Slope Front, *Mar. Chem.*, *35*(1–4), 9–24, doi:10.1016/S0304-4203(09)90005-6.

Levitus, S. et al. (2013), The World Ocean Database, *Data Sci. J.*, *12*(May), WDS229-WDS234, doi:10.2481/dsj.WDS-041.

Nencioli, F., C. Dong, T. Dickey, L. Washburn, and J. C. Mcwilliams (2010), A vector geometry-based eddy detection algorithm and its application to a high-resolution numerical model product and high-frequency radar surface velocities in the Southern California Bight, *J. Atmos. Ocean. Technol.*, *27*(3), 564–579, doi:10.1175/2009JTECHO725.1.

Nicholls, K. W., S. Østerhus, and K. Makinson (2009), … over the continental shelf of the southern Weddell Sea, Antarctica: A review, *Rev. Geophys.*, *47*, 1–23, doi:10.1029/2007RG000250.

Nøst, O. A., M. Biuw, V. Tverberg, C. Lydersen, T. Hattermann, Q. Zhou, L. H. Smedsrud, and K. M. Kovacs (2011), Eddy overturning of the Antarctic Slope Front controls glacial melting in the Eastern Weddell Sea, *J. Geophys. Res. Ocean.*, *116*(11), 1–17, doi:10.1029/2011JC006965.

Orsi, A. H., and C. L. Wiederwohl (2009), A recount of Ross Sea waters, *Deep. Res. Part II Top. Stud. Oceanogr.*, *56*(13–14), 778–795, doi:10.1016/j.dsr2.2008.10.033.

Paolo, F. S., H. A. Fricker, and L. Padman (2015), Volume loss from Antarctic ice shelves is accelerating, *Science (80-.).*, *348*(6232), 327–331, doi:10.1126/science.aaa0940.

Pritchard, H. D., S. R. M. Ligtenberg, H. a. Fricker, D. G. Vaughan, M. R. van den Broeke, and L. Padman (2012), Antarctic ice-sheet loss driven by basal melting of ice shelves, *Nature*, *484*(7395), 502–505, doi:10.1038/nature10968.

Rignot, E., S. Jacobs, J. Mouginot, and B. Scheuchl (2013), Ice-shelf melting around Antarctica., *Science (80-.).*, *341*(6143), 266–70, doi:10.1126/science.1235798.

Ryan, S., M. Schröder, O. Huhn, and R. Timmermann (2016), On the warm inflow at the eastern boundary of the Weddell Gyre, *Deep. Res. Part I Oceanogr. Res. Pap.*, *107*, 70–81, doi:10.1016/j.dsr.2015.11.002.

Saha, S. et al. (2010), The NCEP climate forecast system reanalysis, *Bull. Am. Meteorol. Soc.*, *91*(8), 1015–1057, doi:10.1175/2010BAMS3001.1.

Semper, S., and E. Darelius (2017), Seasonal resonance of diurnal coastal trapped waves in the southern Weddell Sea, Antarctica, *Ocean Sci.*, *13*(1), 77–93, doi:10.5194/os-13-77-2017.

Stewart, A. L., and A. F. Thompson (2013), Connecting Antarctic Cross-Slope Exchange with Southern Ocean Overturning, *J. Phys. Oceanogr.*, *43*, 1453–1471, doi:10.1175/JPO-D-12-0205.1.

Stewart, A. L., and A. F. Thompson (2016), Eddy Generation and Jet Formation via Dense Water Outflows across the Antarctic Continental Slope, *J. Phys. Oceanogr.*, *46*(12), 3729–3750, doi:10.1175/JPO-D-16-0145.1.

Su, Z., A. L. Stewart, and A. F. Thompson (2014), An Idealized Model of Weddell Gyre Export Variability, *J. Phys. Oceanogr.*, *44*(6), 1671–1688, doi:10.1175/JPO-D-13-0263.1.

Timmermann, R., and H. H. Hellmer (2013), Southern Ocean warming and increased ice shelf basal melting in the twenty-first and twenty-second centuries based on coupled ice-ocean finite-element modelling, *Ocean Dyn.*, *63*(9–10), 1011–1026, doi:10.1007/s10236-013-0642-0.

Timmermann, R., S. Danilov, J. Schröter, C. Böning, D. Sidorenko, and K. Rollenhagen (2009), Ocean circulation and sea ice distribution in a finite element global sea ice-ocean model, *Ocean Model.*, *27*(3–4), 114–129, doi:10.1016/j.ocemod.2008.10.009.

VanCaspel, A. (2016), The importance of the western Weddell Sea to Weddell Sea Deep Water formation, University of Bremen.